Journal of Volcanology and Geothermal Research, 27 (1986) 371—397
Elsevier Science Publishers B.V., Amsterdam — Printed in The Netherlands

A MODEL FOR THE TRANSIENT TEMPERATURE EFFECTS OF HORIZONTAL FLUID FLOW IN GEOTHERMAL SYSTEMS

J.P. ZIAGOS[1] and D.D. BLACKWELL[2]

[1]*551 Malbec Court, Pleasanton, CA 94566, U.S.A.*
[2]*Department of Geological Sciences, Southern Methodist University, Dallas, TX 75275, U.S.A.*

(Received December 30, 1983; revised and accepted June 3, 1985)

ABSTRACT

Ziagos, J.P. and Blackwell, D.D., 1986. A model for the transient temperature effects of horizontal fluid flow in geothermal systems. *J. Volcanol. Geotherm. Res.*, 27: 371—397.

A characteristic temperature versus depth (*T-D*) profile is observed in various geothermal environments. Particular features of the *T-D* profile can be explained in terms of a simple time-dependent two-dimensional (x, z) hydrothermal model. In this model a hot fluid is constrained to flow along a thin aquifer buried at a depth l from the surface with conductive heat transfer into the rocks both above and below the aquifer. In many geothermal systems transient changes in the flow patterns occur whose thermal effects can be described in terms of this model. The mathematical representation is that of a layer of thickness l over a half-space with specified temperature on the surface and variable temperature along the interface. An approximate analytical solution is derived using the Laplace transform solution technique and compared to a numerical Fourier transform solution. This approximate analytical solution is computationally simple and can be expressed in terms of key parameters of the fluid flow system. These key parameters are useful in understanding and exploring the sometimes complex hydrology of geothermal systems. Because of the simple computational form, the solution is easily implemented in an inverse solution scheme. Two *T-D* profiles, one from the Oregon Cascade Range and one from Arizona, are forward and inverse modeled, respectively. Fluid flow, velocity, time since initiation of flow, and background gradient are estimated parameters.

INTRODUCTION

Temperature-depth measurements are often used in the exploration of geothermal systems and their subsequent evaluation and production. Interpretation of the measured temperature-depth profiles is often based on the assumption of conductive heat transfer outside the main part of the geothermal system (see Brott et al., 1981), and on temperatures that increase linearly with depth. Many temperature-depth (*T-D*) profiles do not exhibit an increasing temperature with increasing depth, however, and over some depth ranges in a hole, temperatures may decrease or remain constant

0377-0273/86/$03.50

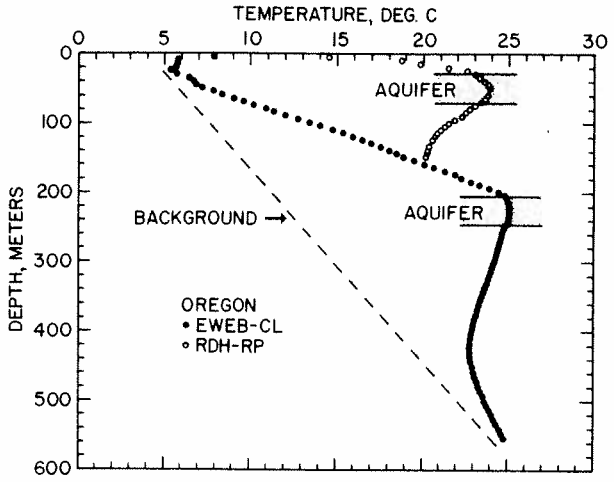

Fig. 1. Examples of characteristic inverted temperature-depth profiles from the Cascade Range in Oregon (Blackwell et al., 1982) demonstrating the linear to inverted to linear characteristic shape that will be modelled in this paper.

(isothermal) with increasing depth. A characteristic temperature-depth profile has a linear increase of temperature at shallow depth and a decrease in temperature at greater depth (negative or inverted geothermal gradient) (G. Bodvarsson, 1973; Ziagos and Blackwell, 1981; and G.S. Bodvarsson et al., 1981). In some cases, at greater depth, the geothermal gradient may become positive so that an increase in depth produces an increase in temperature again. Figure 1 shows two examples from the northern Oregon Cascade Range (Blackwell et al., 1982). As G. Bodvarsson (1973) points out, these temperature inversions can be of diagnostic value in determining the thermal and fluid flow structure within a geothermal system.

Such temperature inversions have been explained as the result of fluid flow within a thin horizontal or shallowly dipping fracture or aquifer (G. Bodvarsson, 1969, 1973). However, the analytical model discussed by G. Bodvarsson (1969) did not include the effect of the surface of the earth. In this paper, a model for the interpretation of these characteristic *T-D* profiles will be presented that includes the surface of the earth as a boundary condition. The identifying feature of these *T-D* profiles is the characteristic smooth change in temperature with depth (which can be matched using the complimentary error-function as described below) in the region below the inferred aquifer zone as shown in Fig. 1. Modeling such profiles allows an estimate of time since the initiation of fluid flow. The inverted part of the *T-D* curves contains this temporal information. Other parameters of interest can also be obtained from interpretation of these sorts of curves. Other physical explanations of inverted *T-D* curves are discussed by G. Bodvarsson (1973), and may occur in areas where the flow pattern is more complicated than that of single aquifer between two impermeable layers.

The physical model presented here to explain the observed inverted part of the *T-D* profiles is that of flow of thermal water along a discrete confined aquifer at some depth below the surface of the earth. The rocks are assumed to be impermeable above and below the aquifer and the heat transfer is assumed to occur by conduction only. A schematic diagram of the geometry is shown in Fig. 2b. The horizontal or shallowly dipping aquifer is charged at its intersection with a vertical or steeply dipping feeder aquifer and the thermal fluid moves down the piezometric gradient confined to the thin aquifer. The thermal effects of the feeder aquifer are ignored because a uniform background gradient is assumed to exist in the half-space before initiation of water flow. The horizontal flow velocity is considered constant and the aquifer is assumed to be thin with respect to its depth below the surface of the earth.

The solution first proposed by G. Bodvarsson (1969) is that of a thin horizontal aquifer (a planar heat source) in a whole-space. The solution to a very similar problem appears in Carslaw and Jaeger (1959, p. 396). This particular solution is for a semi-infinite space ($z \geqslant 0$) in contact with a well-stirred fluid (this means that the fluid temperature is constant throughout the fluid and thus there is no thermal boundary layer) at $z \geqslant 0$. This model is also important in the modeling of the injection of steam or hot fluids into petroleum reservoirs. A numerical treatment may be found in Chase and O'Dell (1973). Bodvarsson's solution allowed him to use the *T-D* profile to calculate estimates of the time since water flow began and the average flow in mass per unit time per unit length measured perpendicular to the x-z plane.

This type of model has also been applied to the study of reinjection in geothermal production environments by various investigators; for example see G. Bodvarsson (1972); Gringarten and Sauty (1975); and G.S. Bodvarsson and Tsang (1982). These models include fluid movement through fractures in producing geothermal systems where the advance, in time and space, of the cold reinjected fluid is very important in determining the longevity of the reservoir.

The model presented in this paper includes the effect of the surface of the earth at a height l above the aquifer. If the aquifer is close to the surface, in a relatively short time, the region between the aquifer and the surface is heated to a constant gradient by energy lost from the aquifer. The region below the heat source takes a much longer time to reach steady-state. Thus inverted *T-D* curves of the type shown in Fig. 1 are produced. Including the surface condition in the model, however, creates added complexity such that an analytical solution is precluded. G.S. Bodvarsson et al. (1981, 1982) solve a very similar problem; their solution, however, requires use of a numerical Laplace inversion for each desired use. The difference is that they assume that at some distance below the aquifer the temperature is fixed (by a deeper aquifer for example), and therefore take this fixed temperature as a boundary condition. In this paper the region below the aquifer is assumed to

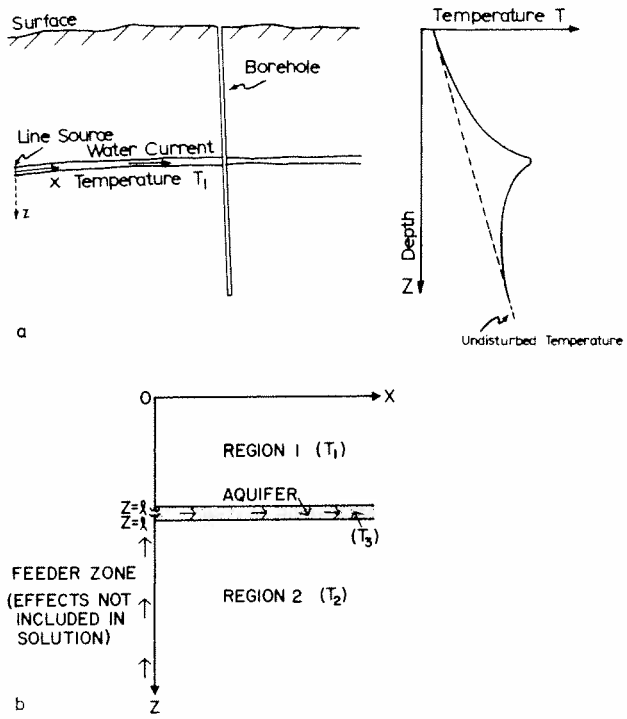

Fig. 2. a. Schematic of geologic model proposed to explain inverted *T-D* profiles (from G. Bodvarsson, 1973). b. Mathematical representation of model showing coordinate frame (x-axis is horizontal and positive to the right, z-axis is positive downward).

be a semi-infinite half-space and temperatures are allowed to reach background values as the conduction of heat should dictate. We have derived an approximate analytic solution for this model that is easy to use for forward or inverse modeling. Of course, the solution of G.S. Bodvarsson et al. (1981, 1982) should approach our solution as the depth of the lower boundary in their model approaches infinity. The solution of G.S. Bodvarsson et al. (1982), since it depends on a numerical Laplace inversion program, is more difficult to apply. The *T-D* profiles that we have observed are compatible with our model (see Fig. 2) and do not warrant the additional complexity of the numerical solution. The inclusion of their lower boundary as a parameter also complicates the interpretation by assuming a priori knowledge of the depth at which the background temperature is to be specified. In most geothermal systems this depth, even if it exists, is not known.

LAPLACE TRANSFORM SOLUTION

Description of the model

The mathematical representation of the physical model presented above is that of a layer of thickness l, over a half-space. The surface of the earth is at

$z = 0$ with z positive downward. The model is two-dimensional (x and z) so that a temperature cross-section at any y, the dimension not shown in Fig. 2, would be identical. The boundary at $x = 0$ is an axis of symmetry and therefore solutions calculated in the quarter-space $x \geqslant 0$ and $z \geqslant 0$ will be sufficient. The fluid is constrained to flow along the boundary at $z = l$, with the input point at $x = 0$ and the flow moving in the positive x-direction. The parameters for the fluid include its heat capacity, thermal conductivity, density and velocity of flow. The thermal parameters for the rock within the layer and in the half-space are thermal conductivity, density and heat capacity. These parameters are assumed to be constant with respect to space, time and temperature. The initial temperature (i.e. at time = 0) is zero throughout the model; this assumption facilitates the later superposition of a background gradient and surface temperature. The temperature effects caused by the fluid rising vertically along the z-axis up to the recharge point of the thermal aquifer at $z = l$, $x = 0$ are not included in the model.

Assumptions

Two basic assumptions are made in the derivation of the differential equations that simplify the mathematics of the solution. The first assumption is that the aquifer is negligible in thickness when compared to the layer thickness (l). Mathematically the thickness is zero and the adjustments for finite layer thickness are incorporated into the fluid mass per unit area parameter.

The second assumption is that horizontal conduction is negligible. This assumption is not unusual (see Carslaw and Jaeger, 1959, p. 392) and can be justified on theoretical and practical arguments. It is possible to relate this assumption to the value of the Peclet number (*Pe*) for this problem. Chase and O'Dell (1973), and Andrews et al. (1981), find that $Pe \geqslant 100$ ensures errors in temperature less than 1% near the propagating warm front. For times of flow after the flow front has passed by a particular distance (x-position), the assumption of negligible horizontal conduction introduces no significant error at that x-position.

Differential equations, boundary and initial conditions

The temperatures of the rock above and below the aquifer are governed by the one-dimensional heat conduction equation (see Appendix A for a listing of symbols used in this paper):

$$\frac{\partial^2 T}{\partial z^2} = \frac{1}{\kappa} \frac{\partial T}{\partial t} \tag{1}$$

The differential equation that must be satisfied within the fluid (or more precisely along the boundary between the regions above and below the aquifer) involves equating energy fluxes across the boundary to the net change in temperature of the fluid, i.e.:

$$q_1|_{z=l} - q_2|_{z=l} = C_f \rho_f a \left[V_f \frac{\partial T_3}{\partial x} + \frac{\partial T_3}{\partial t} \right] \tag{2}$$

(If the fluid is assumed to be well-stirred then $\rho_f a = M_f$ is the fluid mass in contact with the rock per unit area.)

The initial condition is that:

$$T_{1,2,3}(x, z, 0) = 0 \tag{3}$$

The boundary conditions are:

$$T_1(x, 0, t) = 0 \tag{4}$$

$$T_{1,2}(0, l, t) = T_a, t \neq 0 \tag{5}$$

$$T_{1,2}(x, z, t) \to 0 \text{ as } x \to \infty, \text{ for all } t \neq 0 \tag{6}$$

and

$$T_2(x, z, t) \to 0 \text{ as } z \to \infty, \text{ for all } t \neq 0 \tag{7}$$

$$T_1 = T_2 = T_3, \text{ at } z = l, \text{ for all } x, \text{ for all } t \tag{8}$$

Steady-state solution

In the steady-state case a simple analytical solution can be obtained because the heat loss from the aquifer at any x-position is zero into the layer below the aquifer (region 2) due to the fact that the layer has been heated to the aquifer temperature at that point. Thus the heat loss varies only as a function of x in the layer over the aquifer. This heat loss from the fluid in the aquifer must be balanced by the loss of temperature with increasing distance of flow (x) along the aquifer. This energy balance may be expressed as:

$$K_r \left. \frac{dT_1}{dz} \right|_{z=l} = (M_f C_f \rho_f) \frac{dT_3}{dx} \tag{9}$$

but the heat flow out is just equal to the aquifer temperature times the thermal conductivity of the layer divided by the layer thickness, so that:

$$K_r \frac{dT_1}{dz} = -\frac{K_r T_3}{l} \tag{10}$$

Upon solution of the first-order differential equation:

$$T_3(x) = T_a \exp(-\alpha x/l) \tag{11}$$

where T_a is the aquifer temperature at the input point ($x = 0$) and:

$$\alpha = \frac{K_r}{M_f C_f V_f} \tag{12}$$

In this equation, K_r is the thermal conductivity of the rock, V_f is the

velocity of water flow through the aquifer, C_f is the heat capacity of water, and M_f is the mass per unit area of fluid in contact with the rock. The assumption of a thin, isothermal aquifer is embedded in the calculation of M_f which is obtained from a calculation of the pore volume (approximately equal to the fluid mass within the pore space since the fluid density is approximately $1\,g/cm^3$) in the total volume per unit length of the aquifer (thickness is cm × cm × cm × porosity). The aquifer can have a finite thickness and the temperature still be accurately given by eqn. (12) as long as the aquifer is well-mixed and isothermal at each distance. This assumption is addressed in more detail in the discussion section of the paper. The steady-state temperatures at any (x, z) may be calculated from eqn. (11). The surface heat flux in steady-state would be:

$$q(x, 0) = q_0 \exp(-\alpha x/l) \tag{13}$$

where

$$q_0 \equiv K_r T_a / l \tag{14}$$

the maximum heat flux (at the point of recharge).

Approximate analytic solutions using Laplace transform

The period of time of active fluid flow required to reach steady-state in the layer below the aquifer is very large. Thus before steady-state can be reached the flow regime may change due to sealing of the input conduit by mineral deposition or due to tectonic or volcanic events. So a solution is needed which includes the effect of time. The transform solution can be inverted analytically if the assumption is made that the time of flow is "large", or if it is "small".

Approximate analytical solutions to eqns. (1)—(8), which are valid at either short or long times at distances behind the fluid flow front, can be obtained by first taking the Laplace transform with respect to time. The transforms of eqns. (1) and (2) are:

$$\frac{\partial^2 \bar{T}}{\partial z^2} = s^2 \bar{T} \tag{15}$$

and

$$\frac{d\bar{T}_3}{dx} + p\,\frac{\bar{T}_3}{V_f} = \alpha \left(\left.\frac{\partial \bar{T}_1}{\partial z}\right|_{z=l} - \left.\frac{\partial \bar{T}_2}{\partial z}\right|_{z=l} \right) \tag{16}$$

where the bar over the temperature symbol represents the transform and p is the transform variable with:

$$s^2 \equiv p/K_r \tag{17}$$

Appendix B contains details of the solution method and approximations.

The short-time approximate solutions are:

$$T_{1(\mathrm{sts})}(x, z, t) = T_a \left[\sum_{n=0}^{\infty} \left\{ \mathrm{ERFC} \left(\frac{(2n+1)l - z + 2\alpha x}{(4\kappa t')^{1/2}} \right) - \mathrm{ERFC} \left(\frac{(2n+1)l + z + 2\alpha x}{(4\kappa t')^{1/2}} \right) \right\} \right] \tag{18}$$

$$T_{2(\mathrm{sts})}(x, z, t) = T_a \, \mathrm{ERFC} \left(\frac{2\alpha x + z - l}{(4\kappa t')^{1/2}} \right) \tag{19}$$

and

$$T_{3(\mathrm{sts})}(x, l, t) = T_a \, \mathrm{ERFC} \left(\frac{2\alpha x}{(4\kappa t')^{1/2}} \right) \tag{20}$$

where

$$t' = t - t_0 = t - x/V_t \tag{21}$$

It is interesting to note that the short-time surface heat flux is:

$$q_{(\mathrm{sts})}(x, 0, t) = \frac{2T_a}{(\pi\kappa t')^{1/2}} \sum_{n=0}^{\infty} \exp(-\eta^2) \tag{22}$$

where

$$\eta \equiv \frac{(2n+1)l + 2\alpha x}{(4\kappa t')^{1/2}} \tag{23}$$

The long-time approximate solutions are:

$$T_{1(\mathrm{lts})}(x, z, t) = T_a \exp(-\alpha x/l) \sum_{n=0}^{\infty} \left[\mathrm{ERFC} \left(\frac{(2n+1)l - z + \alpha x}{(4\kappa t'')^{1/2}} \right) - \mathrm{ERFC} \left(\frac{(2n+1)l + z + \alpha x}{(4\kappa t'')^{1/2}} \right) \right] \tag{24}$$

$$T_{2(\mathrm{lts})}(x, z, t) = T_a \exp(-\alpha x/l) \, \mathrm{ERFC} \left(\frac{\alpha x + z - l}{(4\kappa t'')^{1/2}} \right) \tag{25}$$

and

$$T_{3(\mathrm{lts})}(x, l, t) = T_a \exp(-\alpha x/l) \, \mathrm{ERFC} \left(\frac{\alpha x}{(4\kappa t'')^{1/2}} \right) \tag{26}$$

where

$$t'' = t' - \frac{\alpha l x}{3\kappa} = t - x/V_f - \alpha l x/3\kappa \tag{27}$$

As $t \to \infty$, $T_{3(\mathrm{lst})}(x, l, t) \to T_a \exp\{-\alpha x/l\}$ which is eqn. (11) of the steady-state solution. It should be noted that the main difference between the short- and long-time approximate solutions is that the time function shifts from t' to t''. The implication of these time shifts will be discussed in a following section.

NUMERICAL SOLUTION USING FOURIER TRANSFORM

Description

In order to determine the range of parameters over which the approximate solutions obtained by the Laplace transform technique are useful, a numerical solution was constructed using the Fourier transform of the differential equations. The Fourier transform technique is used instead of a Laplace inverter for two reasons. The Fourier transform technique provides spectral information about the solution that is unavailable with the Laplace inversion technique and the discrete Fourier transform computer algorithm is easier to use and more readily available. The solution has the same form as that of the equations in Appendix B for the Laplace solution except that: (1) the transform variable is $\beta = (-\mathrm{i}\omega/\kappa)^{1/2}$ instead of $p = (\omega/\kappa)^{1/2}$; and (2) because of the limitations imposed on the solution by the use of the discrete Fourier transform, the flow of water has to be turned on (at $t = 0$) and then off (at some specified time), i.e., the spectrum was multiplied by an equivalent SINC function. In other words, the limitation of the FFT technique is that the boundary conditions must be periodic. So in order to solve the problem, the effect of a cycle of heating by hot fluid flow followed by a cycle of cooling to background temperatures must be followed. Both cycles must be carried out for a time period long enough for the temperature build up (or decrease) to reach the steady-state values after (or before) the hot flow began. Because the cooling part of the cycle is of no interest, many extraneous calculations are required by this solution. Nevertheless, since the approach to the problem is completely different, the Laplace solution in the previous section can be checked.

The spectrum

From Appendix B the solution in the transform domain along the boundary at $z = l$ is:

$$\tilde{T}_3(x, z, \omega) = T_a \tilde{f}(\omega) \exp\left\{-\left(\alpha\beta[\cot(\beta l) - 1] - \frac{\mathrm{i}\omega}{V_f}\right)x\right\} \tag{28}$$

where

$$\alpha = K_r/M_f C_f V_f \tag{29}$$

$\tilde{f}(\omega)$ can be any arbitrary transformed time history of the water flow, in this case a SINC function.

The solutions for the upper and lower regions are:

$$\tilde{T}_1(x, z, \omega) = \tilde{T}_3 \frac{\sin(\beta z)}{\sin(\beta l)} \tag{30}$$

$$\tilde{T}_2(x, z, \omega) = \tilde{T}_3 \exp\{-\beta(z - l)\} \tag{31}$$

Time domain

The inverse Fourier transform of eqns. (28), (30) and (31) was accomplished by digitizing in ω and applying a numerical FFT algorithm. Conditions at $\omega = 0$ were calculated with L'Hospital's rule. Comparison of this solution with the approximate analytical solutions required that the heated water flow along the horizontal aquifer at a constant rate. Therefore $f(\omega)$ is a SINC function. The end time of the square-wave is some time after the times of interest, yet not so far such that aliasing would occur. The water flow is assumed to commence at $t = 0$. Typical temperature and surface heat

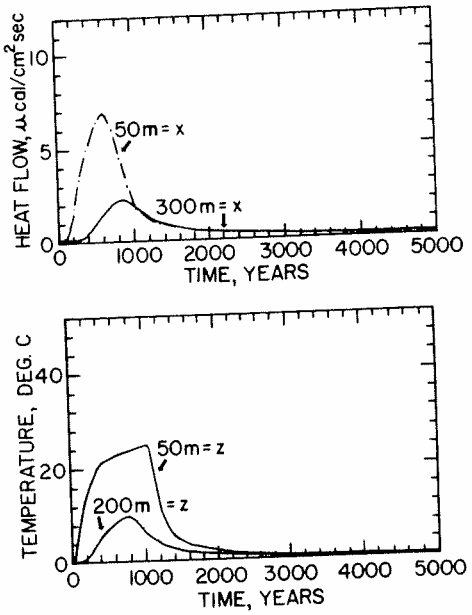

Fig. 3. (top): Surface heat flow as a function of time generated by the numerical FFT solution at different x positions. Other parameters are: $V_f = 1$ m/yr, $\alpha = 1.26$, $K_r = 4$ mcal/cm-s-°C, $t = 200$ yr, $T_a = 50$°C, background gradient = 100°C/km, surface-intercept temperature = 0°C, aquifer depth = 100 m. (bottom): Temperature at $x = 50$ m; other parameters are same as above. These figures represent 1 complete cycle used in the FFT solution.

flow time histories are shown in Fig. 3. This figure shows the full cycle of heating and cooling that must be used to obtain the FFT solution, even though the cooling sections of the curve are not physically useful. The cooling times must be long enough that the wrap-around (temperature at $t = 0$) is as near zero as possible.

Comparison

Once the temperature history is calculated for a particular (x, z) position then the process is repeated at new coordinates. Calculations continue until a complete temperature history is available at the required number of different x- and z-positions. If there are n z-positions and m x-positions to be evaluated then $m \times n$ inverse FFT's are needed. This method is not the computationally most efficient technique for this type of calculation because the continuous time history is not usually needed. Normally only five or six discrete time points are of interest, but we have only used this solution to check the approximate analytical Laplace transform solution.

This numerical solution was compared to an exact solution (at $x = 0$) for a range of different time and depth values. The proper choice of water flow time versus total time (discretization interval times number of intervals) was very crucial to the overall error. In practice this error could be reduced to one part in 10^4 for any time at any $z \leqslant 2l$ at $x = 0$. Also, the numerical solution was compared to the exact steady-state solution. The temperatures matched within 1 part in 10^4.

COMPARISON OF NUMERICAL FOURIER TRANSFORM SOLUTION WITH THE APPROXIMATE LAPLACE TRANSFER SOLUTIONS

Method

The long-term Laplace transformation solution is computationally simple and easy to apply to actual geophysical data. However, it is an approximation, and the degree of approximation needs to be evaluated. The error between the approximate long-time Laplace transformation solution and the numerical Fourier transform solution is demonstrated in Fig. 4. These temperature-depth profiles were calculated at a fixed time (200 yr), with a fixed flow velocity of 1 m/yr, and for different x-positions away from the source ($x = 0$) of the heated fluid. The error of the long-time Laplace solution increases as the x-distance increases because the relative time difference at the greater x-distance (time since passage of the thermal front at that point) is less and so the long-time approximate solution is not applicable. For example, at $x = 60$ m (and 200 yr of flow) the relative time since passage of the thermal front is only 140 yr (at the flow velocity of 1 m/yr) and the long-time approximate solution is not accurate.

Therefore, the range of parameters for which the approximate Laplace transform solutions are valid is of interest. The method used to explore this valid range involved comparing the Fourier transform numerical solution to

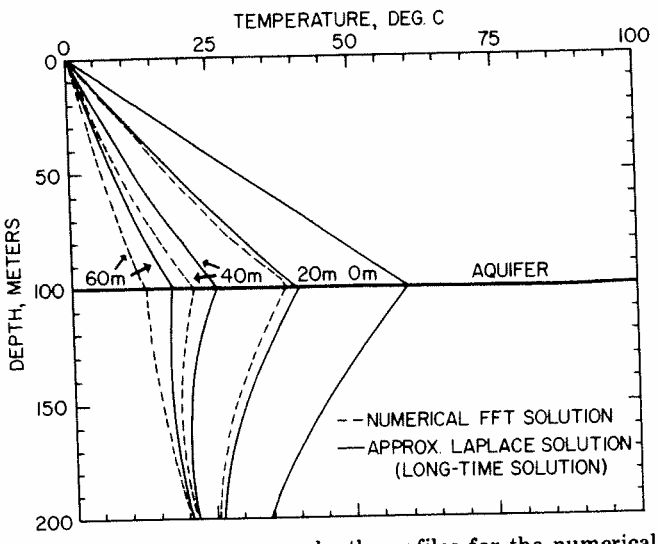

Fig. 4. Temperature versus depth profiles for the numerical (FFT) solution compared to the long-time Laplace approximate solution at $t = 200$ yr at different x-positions. Other parameters are the same as those used in Fig. 3. At $x = 0$ the solutions are identical and as the x-distance increases the difference between the two solutions increases. A linear background temperature increase of 100°C/km has been added to the calculated temperatures.

the long-time Laplace transform approximation for a large range of geophysically realistic values starting at $t = 0$. This calculation was made at $z = l$ (along the aquifer) for there the largest error is realized (as shown in Fig. 4). The difference between the two solutions was calculated throughout the time range of interest and the maximum error was found. At very large times the difference was used as an estimate of the background error of the Fourier transform numerical method for at these times the long-time Laplace transform approximation is exact.

Results

If the temperature histories of a particular point along the aquifer are plotted a characteristic pattern emerges as demonstrated for one particular parameter set in Fig. 5. The FFT numerical solution and the Laplace long-time approximation give very different results from the time hot water first reaches a particular position (x value) until some characteristic "critical time" (t_c) is reached. Subsequently, errors increase again to some maximum value (remaining relatively small) and then decrease. Finally, the temperature histories match very well at very large times with the difference at this stage attributed to the numerical error (wrap around) in the FFT technique. This same error can be seen at very small times near the origin and is caused by aliasing (also demonstrated by the nonzero values of heat flow and temperature shown in Fig. 3 at long times). The three important factors are: the time to reach first intersection, the maximum error after that time, and the background error. For a range of parameters that are geophysically reasonable

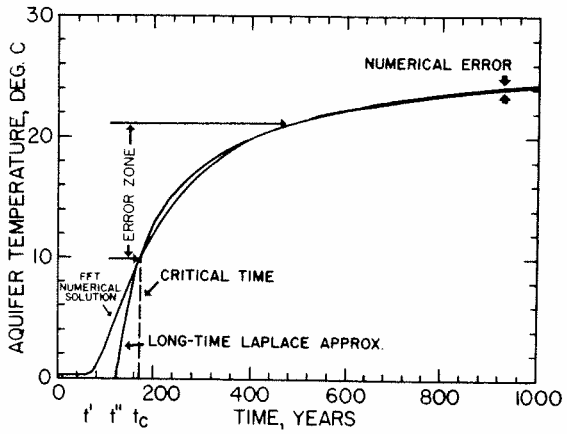

Fig. 5. Aquifer temperature as a function of time for the long-time Laplace transform approximate solution and the numerical FFT solution. This figure is a specific example ($z = l = 100\,\text{m}$; $x = 40\,\text{m}$; $\alpha = 1.26$) of a general effect. The error in aquifer temperature never exceeds 10% after the critical time (t_c) for a broad range of parameter selections. Other parameters are the same as used in Fig. 3. The parameter t' is the time from initiation of flow for the water to reach a particular x distance. The parameter t'' is the corrected time of initiation of water flow for the minimum error using the Laplace long-time solution.

and typically used in applications, the maximum error does not exceed 10% and the background error is typically less than 1%.

The meaning of the time-shift introduced into the long-time approximate solution [see eqns. (24)—(27)] is shown in Fig. 5. In order to best match the true solution (FFT solution) for this set to parameters, the time at which the approximate solution is turned-on (t'') was set to 114 yr. This time-shift is a function of the parameters of the problem and is easily computable [eqn. (27)]. The critical time is the time after which computations using the long-term Laplace transform solution produces less than 10% error in aquifer temperature.

The functional relationship between the various parameters and t_c is not clear from data collected by varying parameters. A clearer understanding emerges if the parameters of length and time are normalized. Figure 6 demonstrates the relationship between normalized horizontal distance as a function of normalized critical time. (The time has been adjusted to the time it takes for the heated water to reach the position x; t'.) Given an α, x, and l then a critical time may be calculated. Also, given a time, a critical distance may be calculated. This relation works for a parameter range which covers the regions of geologic interest, but has not been tested for the entire parameter continuum.

As an example of the use of Fig. 6 consider the *T-D* profiles presented in Fig. 4. Since the time since flow started is fixed at 200 yr, the long-time approximation should be good (i.e. less than 10% error) for x-positions less than 55 m. Conversely, if $x = 40\,\text{m}$ is fixed, the long-time approximate solution will be good at times greater than 150 yr.

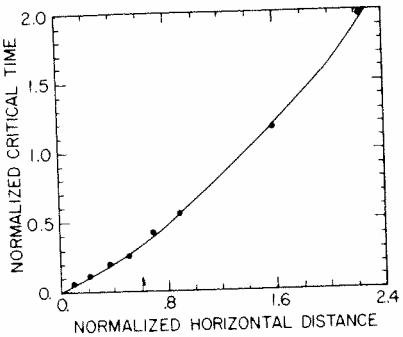

Fig. 6. Normalized critical time: $t_{nc} = (t_c - x/V_f)\kappa/l^2$ versus normalized horizontal distance: $x' = \alpha x/l$. Given a set of parameters α, V_f, l, K_r, and x; a critical time t_c can be derived such that the error in using the long-time Laplace approximation is less than 10%.

APPLICATION AND DISCUSSION

Introduction

The example shown in Fig. 4 and those discussed in the last part of the paper include the superposition of a linearly increasing temperature as a function of depth (constant geothermal gradient), and in some cases a constant surface temperature, on the temperature field calculated from the solution to the flow model. The flow solution is not effected by this superposition. The examples are calculated in this way to more realistically simulate the field situation where the thermal effects of the aquifer flow will be superimposed on the existing background temperature field.

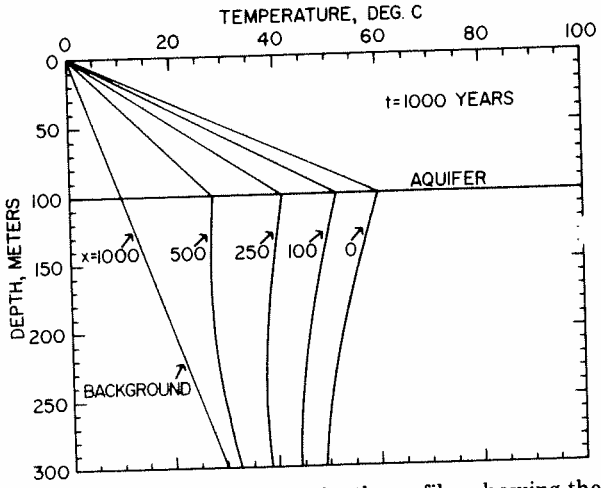

Fig. 7. Temperature versus depth profiles showing the behavior of the long-time approximate solution at different x-positions (in m) at $t = 1000$ yr. Other parameters are: $l = 100$ m, $V_f = 1$ m/yr, $T_a = 50^\circ$C, $K_r = 4.0$ mcal/cm-s-$^\circ$C, background gradient = 100°C/km, aquifer thickness = 10 m, $\alpha = 1.26$ and surface temperature intercept = 0°C.

The results from the long-time approximation may be viewed graphically in several different ways. Temperature versus depth at different x positions (in meters) at one time (1000 yr) for a typical set of parameters are shown in Fig. 7. A background gradient of 100°C/km has been added to the solution. The characteristic shape of the *T-D* profile is evident in these solutions. The critical distance and time are not necessarily within the range for a good approximation for this parameter set because these *T-D* profiles are for demonstration purposes only. The short time behavior of this solution produces characteristic patterns as demonstrated in Fig. 8, where the solutions are displayed as temperature versus depth for $x = 0$, at different times. (Care must be taken to avoid too short a time for $x \geqslant 0$.) Also, other possible graphic displays are of interest, for example the surface heat flux at ($z = 0$) for all x at different times, and the aquifer temperature at ($z = l$).

In general, the particular application of this model is dependent on which input parameters are known. Forward or inverse modeling can be applied to either single or multiple hole data. If fluid flow parameters such as maximum aquifer temperature (from fluid geochemistry for example), heat loss rates, and thickness and porosity of the aquifer are known from independent data, then more information can be obtained from a single *T-D* curve. Parameters such as background gradient, age of fluid flow, fluid flow rate, and x-position may be resolvable. In the worst case, where only a single *T-D* profile (and no other information) is available, fluid flow rate, maximum aquifer temperature and the x-position are not resolvable. Probably the most important application of the solution is to identify the temperature disturbances caused by the known fluid motion, so that the background gradient can be estimated. Two other types of data may be modeled; the maximum aquifer temperature versus x-position or the surface heat flux versus x-

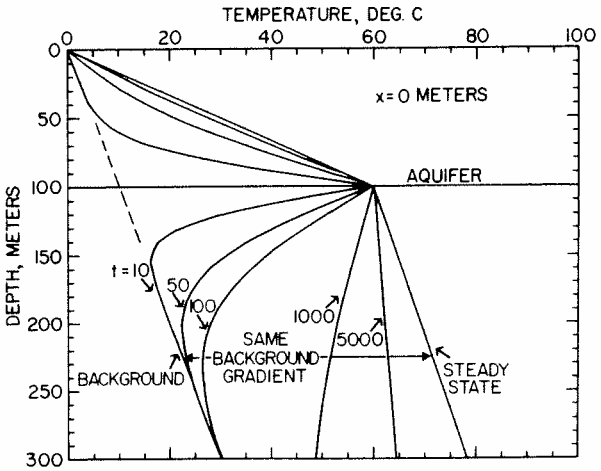

Fig. 8. Temperature versus depth curves at $x = 0$, using the Laplace long-time approximation for different times (in years). Other parameters are the same as used in Fig. 7.

position. This type of modeling demands a multi-hole *T-D* data set. Two examples were chosen to demonstrate some of these modeling ideas. The long-time approximate solution is used in both examples.

Forward modeling of a single T-D curve

Temperature versus depth data, from a hole in Oregon (EWEB-CL) are used as a forward modeling demonstration. The close agreement between calculated and measured data is shown in Fig. 9. The average temperature error is 0.25°C with a maximum error of 1.0°C. The parameters for this model are:

surface temperature	23°C
background gradient	37.5°C/km
temperature anomaly	15.5°C
time since flow onset	860 yr

The thermal conductivity of the rock is 4.0 mcal/cm-s-°C and α was set at 0.13. The nondimensional alpha parameter contains information about the fluid (density, heat capacity, and velocity), the rock (thermal conductivity), and the thickness of the aquifer. If the materials properties can be estimated from other sources of information, then the fluid velocity may be estimated. In this example the x-position was set to zero because it cannot be determined from a single *T-D* data set. The close match between the two *T-D* curves is encouraging, though these model parameters are not unique. An investigation into the uniqueness of any forward modeling approach demands numerous iterations. An effective technique for doing this investigation is the so-called generalized linear inverse technique.

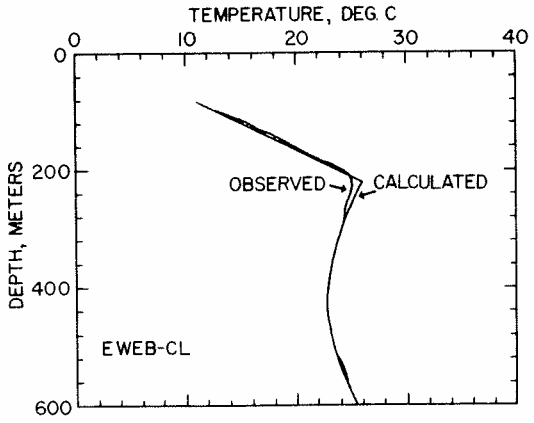

Fig. 9. Observed and calculated temperatures for well EWEB-CL in Oregon (using the Laplace long-time approximate solution). Match was achieved using forward modeling. Parameters for model are given in the text.

hole *T-D* data set. Two
ese modeling ideas. The
ıples.

Oregon (EWEB-CL) are
lose agreement between
The average temperature
The parameters for this

3°C
7.5°C/km
5.5°C
60 yr

m-s-°C and α was set at
s information about the
(thermal conductivity),
perties can be estimated
locity may be estimated.
it cannot be determined
n the two *T-D* curves is
unique. An investigation
ach demands numerous
stigation is the so-called

B-CL in Oregon (using the
ed using forward modeling.

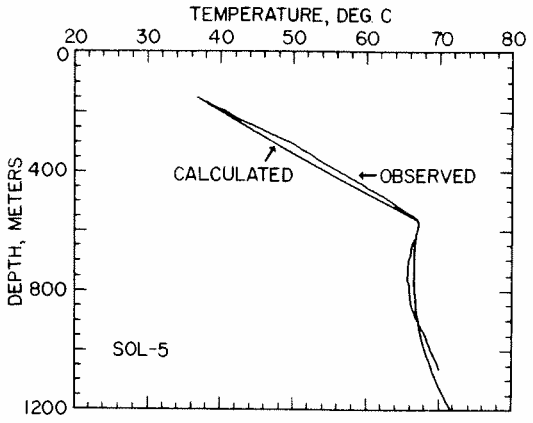

Fig. 10. Observed and calculated temperatures for well SOL-5 in Arizona (using the long-time approximate solution). Match was achieved with an automated inverse modeling procedure. Parameters for model are given in the text.

Inversion modeling of a single T-D curve

Reiter and Shearer (1979) have published *T-D* profiles for the Safford Valley in southeastern Arizona. A "complicated hydrothermal regime at depth" was the explanation for the inverted temperatures in the SOL-5 bore hole shown in Fig. 10. The characteristic shape of this *T-D* profile make it a likely candidate for a model inversion test.

The technique of generalized linear inversion (GLI) involves the correction of an initial guess by the first term of the Taylor series expansion of the forward model for each parameter (see Jackson, 1972). The process does not always converge and the initial guess must be fairly close to the final estimate. The L_2-norm is minimized when there are more data than parameters. Derivatives with respect to temperature intercept, background gradient, the product αx, the anomaly temperature, and finally the time since the flow was initiated were calculated.

The results of the inversion are presented on Figure 10 with the final parameter selection:

surface temperature	26.3°C
background gradient	35.5°C/km
αx	66 m
temperature anomaly	26.5°C
time since flow onset	3120 yr

If the rock thermal conductivity is 6.5 mcal/cm-s-°C, the fluid density and heat capacity are that of water, and fluid velocity is estimated at 12.5 m/yr, then the x-position is estimated as 200 m. Since the product αx is included in the inversion the velocity of the fluid as well as the other parameters mentioned above trade-off with the x-position so that these parameters are by no means uniquely determined from the data in a single hole. The average

error between the calculated and the observed temperatures was 0.9°C. The maximum error was 2.1°C.

One of the advantages of using the generalized linear inverse technique is that the resolution of the parameters through the resolution matrix as well as the importance of the individual data to the solution through the information density matrix may be evaluated. The resolution matrix calculates the interdependency between the parameters. The information density matrix allows the relative importance of individual *T-D* measurements to be weighed. These matrices were calculated and interpreted for this model and this data set. The individual parameters were strongly independent except for the time parameter. This parameter showed a strong correlation with the surface intercept temperature and the anomaly temperature. Also, there was some interrelationship with the product parameter αx. The *T-D* data of greatest importance are the surface intercept temperature, the maximum temperature before decrease, and the deepest *T-D* value.

DISCUSSION AND CONCLUSIONS

In order to match the observed inverted *T-D* profile and to predict convective parameters an approximate Laplace transform solution that is exact at long times was found for a simple horizontal fluid flow model. Neglecting horizontal thermal conduction limits the applicability of the model to certain parameter values. Within these limits, there exists a further restriction due to the nature of the approximation. In order to quantify this restriction a numerical FFT solution to this model was developed. By comparing the two solutions over a large parameter range, an empirical relationship was found between the critical time and the other parameters. Some of the examples presented show that this restriction is not particularly limiting. After this critical time, the maximum error between the numerical and approximate solutions never exceeded 10% in the cases investigated. Most of the difficulty in finding an exact solution is due to the temperature-time behavior near the propagating thermal front. Since most geothermal systems have been operating for some time, most of the *T-D* profiles to be modeled do not include this short-time behavior.

The approximate solution was used to estimate parameters in two different ways. Using the solution in a forward model procedure, thermal parameters were estimated for a bore hole in Oregon. Since the equations are analytic, they are easily used with a formalized inverse modeling approach. This inverse modeling was done for data in Arizona and thermal parameters were estimated. From this analysis it was found that the time parameter is least resolvable and that the surface, anomaly, and deepest temperatures have the greatest influence on the final solution set.

Temperature inversions are ubiquitous in geothermal systems. Numerous examples of such inverted *T-D* curves from the United States which might be examples of the effect described in the previous sections have been published

in recent years as more and more geothermal systems have been explored. Examples have been described from the Gerlach area in Nevada (Sass et al., 1979), the Baltazor area in Nevada (Hulen, 1983), the Lassen Peak area in California (Beall, 1981), the Desert Peak area in Nevada (Benoit et al., 1982) and the Long Valley caldera in California (Blackwell, 1985).

The temperature-depth curves found in the upper 3 km of wells on the west edge of the Valles caldera (Harrison et al., 1985) may be a good example of this effect. Water moving through the Paleozoic Madera limestone out of the Valles caldera geothermal system at a depth of 700 m heats up the Precambrian basement to a depth of 2—2.5 km. The period of flow has been on the order of 10,000 yr. A spectacular example of a double inversion due to two separate aquifers is seen in a deep hole in the Long Valley caldera (Blackwell, 1985).

There are numerous additional complexities in actual *T-D* curves, of course. A good example of a *T-D* curve showing some of these complexities is illustrated in Fig. 11. Several *T-D* curves from the Walker "0" well near Mt. Lassen, California are shown (Beall, 1981). The curve from 8/8/79 is an equilibrium log while the other log was made shortly after completion of drilling in 1978. The aquifer in this hole is not thin and significant zones of thermal transition (approximately 100 m thick), either thermal boundary layers, or mixing zones, occur above and below the isothermal core of the aquifer (between 425 and 640 m). The extent of the aquifer can be deduced from the fact that major and irregular cooling is shown by the log of 10/25/78 down to 760 m while below that depth the *T-D* log is very similar to the equilibrium log of 8/8/79. Significance fluid loss during drilling

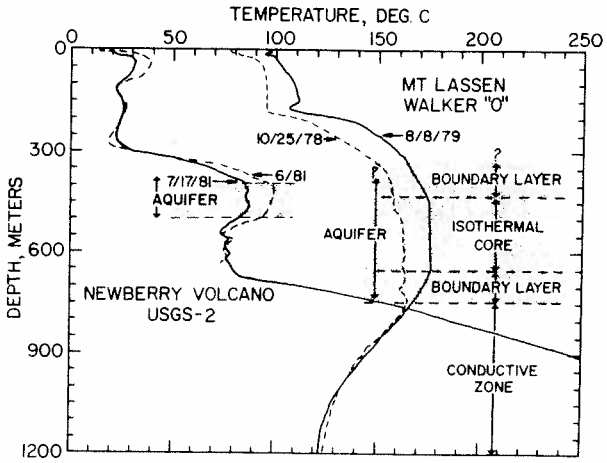

Fig. 11. Examples of temperature inversions in geothermal wells that are more complicated than examples shown in Fig. 1. Data from Walker "0" well are from Beall (1981). Newberry volcano well *T-D* example is an overturn of a type not described by the model in this paper and Walker "0" *T-D* curve is an example of a thick, confined aquifer.

evidently cooled the hole more effectively to that depth by flooding of cooler water into the formation. The extent of the cooling effect outlines the aquifer. In this case the aquifer either extends to the surface, or more likely, the temperatures above 300 m are controlled by convective effects and steam-phase formation within the bore hole. In spite of the departures from the ideal case some information may still be obtained from the section of the *T-D* curve below the aquifer.

In contrast, two temperature logs from a hole in the crater of Newberry volcano, Oregon show a temperature inversion of a very different sort. An equilibrium log made when the hole was at a depth of 610 m and a non-equilibrium log made following subsequent drilling are also shown in Fig. 11 (Blackwell, unpublished log; see also Sammel, 1981). The *T-D* curves are very complex even in the equilibrium case and the transition from high temperature in the aquifer (between 400 and 500 m) to low temperature above and below the aquifer does not have the shape of the model discussed in this paper. In this case the hot aquifer may or may not be separated by thin aquitards from aquifers containing water of much lower temperatures both above and below. A *T-D* curve from the Kileaua volcano in Hawaii (Zablocki et al., 1974) is similar to the Newberry curve above the aquifer although the *T-D* curve may reflect conductive heat transfer below the aquifer.

In a very different type of setting, homogeneous permeable medium, Rayleigh convection may result in temperature inversions. The inversions will become more exaggerated as the Rayleigh number of the flow increases. Such inversions at Wairakei were pointed out by Elder (1965). In this sort of setting *T-D* curves may be found that might be mistaken for long-time examples of the model described in this paper. Knowledge of the geology or results from drilling (including fluid loss zones and the character of the thermal recovery) should make the interpretation of the subsurface conditions possible, however.

A final complication to be discussed here is the confusion of the true nature of the *T-D* curve in a geothermal well by transient drilling effects. Equilibrium *T-D* logs may be required to recognize, and especially to quantitatively interpret, specific cases using the model described in this paper. Benoit et al. (1982) illustrate such a case from the Desert Peak area in Nevada. Immediately following drilling of the 2350 m deep well 29-1 temperature logs showed a broad temperature peak at about 370 m with an inversion amplitude of 2°C. Following establishment of thermal equilibrium over a month later the amplitude of the inversion reached 25°C, the curve was much more peaked, and the inversion started at a depth of 250 m. Cooling of the shallow aquifer was not obvious on the nonequilibrium *T-D* curves because the shallow aquifer was behind the surface casing and so there was no fluid invasion. Interpretation of the thermal conditions in this well based on the initial nonequilibrium logs would not have been correct (Benoit et al., 1982).

The main usefulness of the model described in this paper is the insight into temporal and special variations in fluid flow in geothermal systems that may be obtained from, first qualitatively and, second, quantitatively applying the model to exploration data. The examples discussed above show that this type of phenomenon is common to geothermal systems. The examples also show some types of information that can be obtained from modeling these types of *T-D* curves. The common occurrence of these types of curves emphasizes the transient nature of fluid flow in geothermal systems. The timescales of flow changes are indicated by the ages of flow determined from the analysis of the curves which range from a few hundred to a few thousand years.

The results obtained from applying the model discussed in this paper can be used directly in the exploration of geothermal systems. Shallow hot water flow in confined aquifers has often caused confusion in the interpretation of geological and geophysical exploration data. The broad scale and intense nature of the shallow systems often effectively mask the deeper, hotter, systems which are of main exploration interest. Once the phenomenon has been recognized, however, drill holes deep enough to evaluate the thermal conditions below the shallow aquifer must usually be the exploration technique. An application of this sort has already been made by Eckstein and Cik (1982) for the Momotombo geothermal area in Nicaragua. An example of exploration utilizing this model in a qualitative sense has been described by Benoit et al. (1982) at the Desert Peak, Nevada geothermal system. The system there is complicated by the fact that leakage occurs into three or more areally distinct, shallow aquifers. The complicated subsurface conditions have significantly reduced the effectiveness of surface exploration techniques.

Blackwell (1985) has discussed a quantitative application of the model to a multiple hole date set from the Long Valley caldera, California. In that system deep drilling based on surface geophysics and shallow drill holes have encountered two thermal aquifers with maximum temperatures of 175°C, but not the deep, hot, system feeding the shallow aquifers (at 210 + °C based on geochemical interpretations). Flow parameters of the system based on the shallow aquifer model and on hydrologic studies by Sorey et al. (1978) are in remarkable agreement. The ages of flow inferred for the two aquifers are about 600 ± 100 yr and 3000 ± 1000 yr. The last major eruptive event in the caldera has been dated at about 600 yr. Thus movement associated with the eruption might have set up conditions that caused the leakage of hot fluid into the shallow east aquifer.

ACKNOWLEDGEMENTS

John Ferguson was especially helpful during derivation of the solutions and helped with the numerical Fourier transform model. The investigation was stimulated by conversations with Richard Benoit and Robert Edmiston.

The authors benefitted greatly from conversations with students and faculty at the Southern Methodist University of Geological Sciences including Wayne Peeples and Eugene Herrin. Research was supported by Grant 81ER10973 from the U.S. Department of Energy program in Basin Energy Science, and by the Geothermal Laboratory of the Institute for the Study of Earth and Man of Southern Methodist University.

APPENDIX A: Nomenclature

Aquifer parameters

V_f = fluid velocity, (m/yr)
T_a = fluid temperature maximum, (°C)
ρ_f = fluid density, (g/cm^3)
C_f = fluid heat capacity, (cal/g°C)
a = aquifer thickness, (m)
M_f = mass per area of fluid in aquifer

Rock parameters

K_r = rock thermal conductivity (mcal/cm-s-°C)
κ = rock diffusivity (m^2/yr)
ρ_r = rock density (g/cm^3)
C_r = rock heat capacity (cal/g-°C)
l = layer-over thickness (m)

Coordinate parameters

x = distance parallel to horizontal aquifer (m)
z = distance perpendicular to horizontal aquifer (m)
t = time since flow initiation, (yr)
t' = time corrected for moveout, (yr) = $t - xV_f^{-1}$
t'' = time corrected for approximate (long-time) = $t' - (\alpha x l)/3\kappa$, (yr)
t_0 = travel time at x, (yr) = x/V_f (yr)

Temperature parameters

$T_1(x, z, t)$ = temperature in layer-over half-space, (°C)
$T_2(x, z, t)$ = temperature in half-space, (°C)
$T_3(x, t)$ = temperature in aquifer, (°C)
T_a = source temperature of aquifer, (°C)

Nondimensional parameters

$\eta = [(2n + 1)l + 2\alpha x]/(4\kappa t')^{1/2}$
$\alpha = K_r/M_f C_f V_f$
$x' = \alpha x/l$
$t_{nc} = (t_c - t_0)\kappa/l^2$

Other parameters

ϵ $= -\alpha s[1 + \coth(sl)] + pV_f$

β $= (-i\omega/\kappa)^{1/2}$

p = Laplace transform variable

$\bar{T}_{1,2,3}$ = bar over, denotes Laplace transformed temperature

Pe = Peclet number $= L_c V_f/\kappa$ (L_c = critical length)

s $= (p/\kappa)^{1/2}$

$\tilde{T}_{1,2,3}$ = tilde over, denotes Fourier transformed temperature

APPENDIX B: Derivation of long- and short-time solutions

Start with the transformed solutions:

$$\bar{T}_1 = (T_a/p)\exp(-|\epsilon|x)\frac{\sinh(sz)}{\sinh(sl)} \tag{B1}$$

$$\bar{T}_2 = (T_a/p)\exp[-|\epsilon|x - s(z-l)] \tag{B2}$$

$$\bar{T}_3 = (T_a/p)\exp(-|\epsilon|x) \tag{B3}$$

where:

$$\epsilon = -\alpha s[1 + \coth(sl)] + pV_f \tag{B4}$$

$$s^2 = p/\kappa \tag{B5}$$

$$\alpha = K_r/M_f C_f V_f \tag{B6}$$

The hyperbolic cotangent term appearing in these solutions is not invertible using standard techniques, but approximate solutions are possible. Start by expanding the hyperbolic cotangent in a Maclaurin series:

$$\coth(x) = \frac{1}{x} + \frac{x}{3} - \frac{x^3}{45} + \ldots + \tag{B7}$$

But this series is only good for $|x| < \pi$. If we look at the hyperbolic cotangent function we find:

as $X \to \infty$, $\coth(X) \to 1$ and,

as $X \to 0$, $\coth(X) \to 0$.

A good approximation for small values of x is $\coth(x) \approx 1/x + x/3$. A good approximation for $\coth(x)$ for large values of x is $\coth(x) \approx 1$. These two approximations upon inversion represent respectively the short-time and long-time behavior of this solution. If the $X/3$ term is neglected in the expansion then another approximation is generated. This is the approximation

presented by Ziagos and Blackwell (1981). Let us now begin to solve eqns. (B1)—(B3) and at the appropriate step insert the approximations. Starting with eqn. (B3):

$$\bar{T}_3 = (T_a/p)\exp\{-|\epsilon|x\} \tag{B8}$$

For the short-time solutions (we designate sts):

$$\coth(sl) \approx 1$$

and therefore eqn. (B8) is now:

$$\bar{T}_{3(\mathrm{sts})} = (T_a/p)\exp\{-pt_0 - 2\alpha s x\} \tag{B9}$$

This inverts to:

$$T_{3(\mathrm{sts})} = T_a\ \mathrm{ERFC}\left(\frac{2\alpha x}{(4\kappa t')^{1/2}}\right) \tag{B10}$$

We apply the sts approximations to the other equations:

$$\bar{T}_{2(\mathrm{sts})} = (T_a/p)\exp[-pt_0 - s(z - l + 2\alpha x)] \tag{B11}$$

upon inversion:

$$T_{2(\mathrm{sts})} = T_a\ \mathrm{ERFC}\left(\frac{z - l + 2\alpha x}{(4\kappa t')^{1/2}}\right) \tag{B12}$$

and for $\bar{T}_1$:

$$\bar{T}_{1(\mathrm{sts})} = (T_a/p)\exp(-pt_0 - 2s\alpha x)\ \frac{\sinh(sz)}{\sinh(sl)} \tag{B13}$$

rewriting:

$$\bar{T}_{1(\mathrm{sts})} = (T_a/p)\exp(-pt_0)\left[\frac{\exp[-s(l - z + 2\alpha x)] - \exp[-s(l + z + 2\alpha x)}{1 - \exp(-2sl)}\right. \tag{B14}$$

using the binomial expansion we get (for large (sl) values):

$$\bar{T}_{1(\mathrm{sts})} = (T_a/p)\exp(-pt_0)[\exp[-s(l - z + 2\alpha x)] - \exp[-s(l + z + 2\alpha x)]]\ \sum_{n=0}^{\infty}\exp(-2nls) \tag{B15}$$

rearranging:

$$\bar{T}_{1(\mathrm{sts})} = (T_a/p)\left[\sum_{n=0}^{\infty}(\exp\{-s[(2n+1)l - z + 2\alpha x]\} - \exp\{-s[(2n+1)l + z + 2\alpha x]\})\right]\exp(-pt_0) \tag{B16}$$

now begin to solve eqns.
approximations. Starting

(B8)

upon inversion:

$$\bar{T}_{1(\mathrm{sts})} = T_a\left[\sum_{n=0}^{\infty}\left\{\mathrm{ERFC}\left(\frac{(2n+1)l-z+2\alpha x)}{(4\kappa t')^{1/2}}\right)\right.\right.$$

$$\left.\left.-\,\mathrm{ERFC}\left(\frac{(2n+1)l+z+2\alpha x)}{(4\kappa t')^{1/2}}\right)\right\}\right] \tag{B17}$$

the heat flux at $z = 0$ for this solution is:

(B9)

$$q_{0(\mathrm{sts})} = \frac{2T_a}{(\pi\kappa t')^{1/2}}\sum_{n=0}^{\infty}\exp(-\eta^2) \tag{B18}$$

(B10)

where $\eta = \dfrac{(2n+1)l+2\alpha x}{(4\kappa t')^{1/2}}$

ions:

Now apply the long-time approximations:

(B11)

$$\bar{T}_{3(\mathrm{lts})} = (T_a/p)\exp(-pt_0 - \alpha sx - \alpha x/l - \alpha s^2 lx/3\kappa) \tag{B19}$$

upon inverting:

(B12)

$$T_{3(\mathrm{lts})} = T_a\exp(-\alpha x/l)\,\mathrm{ERFC}\left(\frac{\alpha x}{(4\kappa t'')^{1/2}}\right) \tag{B20}$$

For $\bar{T}_{2(\mathrm{lts})}$:

(B13)

$$\bar{T}_{2(\mathrm{lts})} = (T_a/p)\exp(-pt_0 - \alpha sx - \alpha x/l - \alpha s^2 lx/3\kappa + sz) \tag{B21}$$

upon inversion:

$$T_{2(\mathrm{lts})} = T_a\exp(-\alpha x/l)\,\mathrm{ERFC}\left(\frac{\alpha x+z-1}{(4\kappa t'')^{1/2}}\right) \tag{B22}$$

$-\exp[-s(l+z+2\alpha x)]\Big]$
$\exp(-2sl)$

(B14)

where: $t'' = t - x/V_f - (\alpha lx/3\kappa)$

and

alues):

$$\bar{T}_{1(\mathrm{lts})} = (T_a/p)\{\exp[-pt_0 - \alpha xs - \alpha x/l - (\alpha plx)/3\kappa]\}\frac{\sinh(sz)}{\sinh(sl)} \tag{B23}$$

upon inversion becomes:

(B15)

$$T_{1(\mathrm{lts})} = T_a\exp(-\alpha x/l)\sum_{n=0}^{\infty}\left[\mathrm{ERFC}\left(\frac{(2n+1)l-z+\alpha x}{(4\kappa t'')^{1/2}}\right)\right.$$

$$\left.-\,\mathrm{ERFC}\left(\frac{(2n+1)l+z+\alpha x}{(4\kappa t'')^{1/2}}\right)\right] \tag{B24}$$

$c]\}$

$-pt_0)$ (B16)

REFERENCES

Andrews, J.G., Richardson, S.W. and White, A.L., 1981. Flushing geothermal heat from moderately permeable sediments. J. Geophys. Res., 86: 9439—9450.

Beall, J., 1981. A hydrological model based on deep test data from the Walker "0" No. 1 well, Terminal Geyser, California. Trans. Geotherm. Resour. Counc., 5: 153—156.

Benoit, W.R., Hiner, J.E. and Forest, R.T., 1982. Discovery and geology of the Desert Peak geothermal field: A case study. Nevada Bur. Mines Geol., Bull. 97, 82 pp.

Blackwell, D.D., 1985. A transient model of the geothermal system of the Long Valley caldera, California. J. Geophys. Res., in press.

Blackwell, D.D., Bowen, R.G., Hull, D.A., Riccio, J. and Steele, J.L., 1982. Heat flow, arc volcanism, and subduction in Northern Oregon. J. Geophys. Res., 87: 8735—8754.

Bodvarsson, G.S. and Tsang, C.F., 1982. Injection and thermal breakthrough in fractured geothermal reservoirs. J. Geophys. Res., 87: 1031—1048.

Bodvarsson, G.S., Miller, C.W. and Benson, S.M., 1981. A simple model for fault-charged hydrothermal systems. Trans. Geotherm. Resour. Counc., 5: 323—327.

Bodvarsson, G.S., Benson, S.M. and Witherspoon, P.A., 1982. Theory of the development of geothermal systems charged by vertical faults. J. Geophys. Res., 87(11): 9317—9328.

Bodvarsson, G. 1969. On the temperature of water flowing through fractures. J. Geophys. Res., 74(8): 1987—1992.

Bodvarsson, G., 1972. Thermal problems in the siting of reinjection wells. Geothermics, 1(2): 63—66.

Bodvarsson, G., 1973. Temperature inversions in geothermal systems. Geoexploration, 11: 141—149.

Brott, C.A., Blackwell, D.D. and Morgan, P., 1981. Continuation of heat flow data: A method to construct isotherms in geothermal areas. Geophysics, 46(12): 1732—1744.

Carslaw, H.S. and Jaeger, J.C., 1959. Conduction of Heat in Solids. Oxford University Press, New York, N.Y., 386 pp.

Chase, C.A. and O'Dell, P.M., 1973. Application of variational principles to cap and basement heat losses. S.P.E. J., 13(4): 200—210.

Eckstein, Y. and Cik, R., 1982. Use of temperature inversion data for determining the age of fracturing in a geothermal area, abstract. EOS, Trans. Am. Geophys. Union, 63: 45.

Elder, J.W., 1965. Physical processes in geothermal areas. In: W.H.K. Lee (Editor), Terrestrial Heat Flow, Geophys. Monogr. Ser., vol. 8. AGU, Washington, D.C., pp. 211—239.

Gringarten, A.C. and Sauty, J.P., 1962. A theoretical study of heat extraction from aquifers with regional flow. J. Geophys. Res., 80: 4956—4962.

Harrison, T.M., Morgan, P. and Blackwell, D.D., 1985. Constraints on the age of heating of the Fenton Hill site, Valles Caldera, New Mexico. J. Geophys. Res., in press.

Hulen, J.B., 1983. Structural control of the Baltazor hot springs geothermal system, Humbolt County, Nevada. Trans. Geotherm. Resour. Counc., 7: 157—162.

Lauwerier, H.A., 1955. The transport of heat in an oil layer caused by the injection of hot fluid. Appl. Sci. Ses., Sect. A., 5: 145—150.

Jackson, D.D., 1972. Interpretationof inaccurate, insufficient and inconsistent data. Geophys. J.R. Astron. Soc., 28: 97—109.

Reiter, M. and Shearer, C., 1979. Terrestrial heat flow in Eastern Arizona, a first report. J. Geophys. Res., 84(11): 6115—6120.

Sammel, E.A., 1981. Results of test drilling at Newberry Volcano, Oregon, and some implications for geothermal prospects in the Cascades. Geotherm. Resour. Counc. Bull., 10(11): 3—8.

Sass, J.H., Zoback, M.L. and Galanis, S.P., 1979. Heat flow in relation to hydrothermal activity in the Southern Black Rock Desert, Nevada. U.S. Geol. Surv., Open-file Rep., 79–1467, 39 pp.

Sorey, M.L., Lewis, R.E. and Olmsted, F.H., 1978. The hydrothermal system of Long Valley caldera, California. U.S. Geol. Surv., Prof. Pap., 1044-A: A1—A60.

Zablocki, C.J., Tilling, R.I., Peterson, D.W., Christiansen, R.L., Kelley, G.V. and Murray, J.C., 1974. A deep research drill hole at the summit of an active volcano, Kilauea, Hawaii. Geophys. Res. Lett., 1: 323—325.

Ziagos, J.P. and Blackwell, D.D., 1981. A model for the effect of horizontal fluid flow in a thin aquifer on temperature-depth profiles. Geotherm. Resour. Counc. Trans., 5: 221—223.